ELSEVIER

Ultrasonics 40 (2002) 617–620

Ultrasonics

www.elsevier.com/locate/ultras

Probing acoustic nonlinearity on lengths scales comparable to material grain dimensions

David H. Hurley *, Ken L. Telschow, David Cottle

Idaho National Engineering and Environmental Laboratory, P.O. Box 1625, Idaho Falls, ID 83415-2209, USA

Abstract

The focus of this presentation is to describe our efforts at laser generation of high frequency surface acoustic waves and detection of the nonlinear contribution in the acoustic near-field of the source. Narrow band acoustic generation is accomplished by interfering two pulsed laser beams at the surface of the sample. A Michelson interferometer, that incorporates a high power microscope objective, is used to detect the acoustic disturbance. Detection near the source combined with high frequency generation (~0.1 GHz) facilitates investigation of fundamental processes of harmonic generation on length scales comparable to grain size dimensions. Published by Elsevier Science B.V.

Keywords: Nonlinear acoustics; Laser acoustics; Surface acoustic waves; Rayleigh waves

1. Introduction

Analysis of the nonlinear response of a material offers the potential for measuring certain material properties more effectively than techniques that assume linear behavior [1]. For instance, previously researchers have successfully related changes in the acoustic nonlinear parameter to changes in microstructural features such as voids, dislocations and dislocations dipoles [2–4]. However, issues related to sensitivity to spatial variations in elastic nonlinear behavior must be addressed before nonlinear techniques obtain equal stature with linear techniques. For example, most nonlinear investigations are limited to measuring material properties averaged over relatively large beam propagation paths, as compared to material grain dimensions, through the sample and hence, rely on mean field theory to interpret experimental results [5]. The wave guiding nature of SAWs allows the generation and detection process to be performed on the same side of the sample which in-turn affords enhanced spatial sensitivity since the acoustic propagation distance is not dictated by the sample's dimensions. In addition, laser generation in the thermoelastic regime offers enhance reproducibility, which facilitates data analysis.

In order to decrease the experimental length scale so as to investigate nonlinear behavior at grain size length scales, higher acoustic frequencies are needed. This can be understood by noting that the spatial coupling rate to higher harmonics is enhanced by increasing acoustic frequency [6]. In the past, adverse effects of increased grain boundary scattering at high frequencies has left this avenue of investigation relative unexplored.

2. Experiment

The experimental setup used to generate surface acoustic waves is shown in Fig. 1. The generation of the ultrasonic disturbance was accomplished by irradiation the sample with a mode-lock pulsed Nd:YAG laser operating at 1.064 μm. A narrow band, surface acoustic wave was produced by interfering two generation beams at the sample surface [7]. The two generation beams were made to spatially overlap with the aid of a cylindrical lens resulting in a generation footprint that was approximately 1 cm in length and 300 μm in width. The fringe spacing, which dictates the center frequency of the surface acoustic wave, is given by

$$\Delta = \frac{\lambda}{2\sin(\varphi/2)} \tag{1}$$

* Corresponding author. Fax: +1-208-526-0690.
E-mail address: hurldh@inel.gov (D.H. Hurley).

0041-624X/02/$ - see front matter Published by Elsevier Science B.V.
PII: S0041-624X(02)00185-3

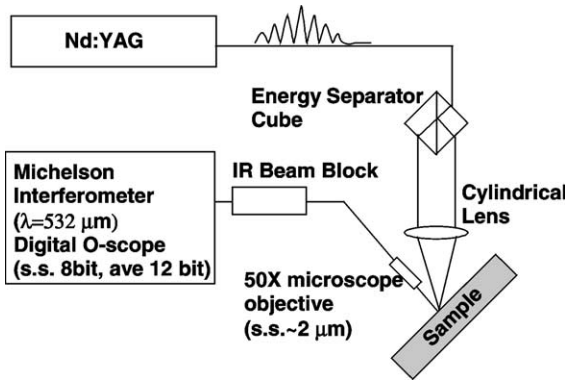

Fig. 1. Experimental setup: a mode-lock pulsed Nd:YAG laser operating at 140 MHz was used to generated a narrow-band pulse train of surface acoustic waves.

where λ is the optical frequency and φ is the angle between the two generation beams. In order to generate large amplitude surface acoustic waves and exploit reproducibility afforded by thermoelastic generation, a pulse train was desired over single pulse operation. This was achieved by disabling the Q-switch and placing a 1/4 wave plate in the oscillator cavity to allow the pulse train, centered at 140 MHz, to exit the cavity. The FWHM of the pulse train, shown in the top graph of Fig. 2, consist of approximately 15 pulses with a pulse duration of approximately 100 ps and a pulse to pulse separation of approximately 7 ns.

In order to ensure that the surface acoustic wave generated by the first pulse is in phase with all subsequent pulses, the acoustic transit time across one fringe should correspond to an integer fraction of the temporal pulse separation. Thus, for the aluminum sample used in this paper, a fringe spacing of approximately 21 μm was required for operation at 140 MHz. Surface acoustic waves generated in this fashion are shown in the middle and bottom graph of Fig. 2. The out-of-plane displacement was detected using a path stabilized Michelson interferometer [8]. The object leg of the interferometer was focused onto the sample with a long-working-distance metallurgical 50× microscope objective with a spot size of approximately 3 μm. The acoustic transit time across the detection spot limits the current experimental setup to an upper bandwidth of approximately 500 MHz. An electro-optic modulator operating at 70 MHz was placed in the reference leg of the interferometer to calibrate the out-of-plane surface displacement.

3. Results

The sample used in the experiment was an aluminum ingot having 6 N purity. The top surface was polished to aid in interferometric detection. The grain structure was revealed by lightly etching the sample in a dilute mixture of hydrochloric and hydrofluoric acid. In order to detect small signals at the second harmonic, the tone-burst nature of this experiment required full utilization of the bit depth of the oscilloscope. A Lecroy oscilloscope, Wavepro 960, was used to acquire the data shown in Fig. 2. The single shot bit depth is 8 and 14 bits math-

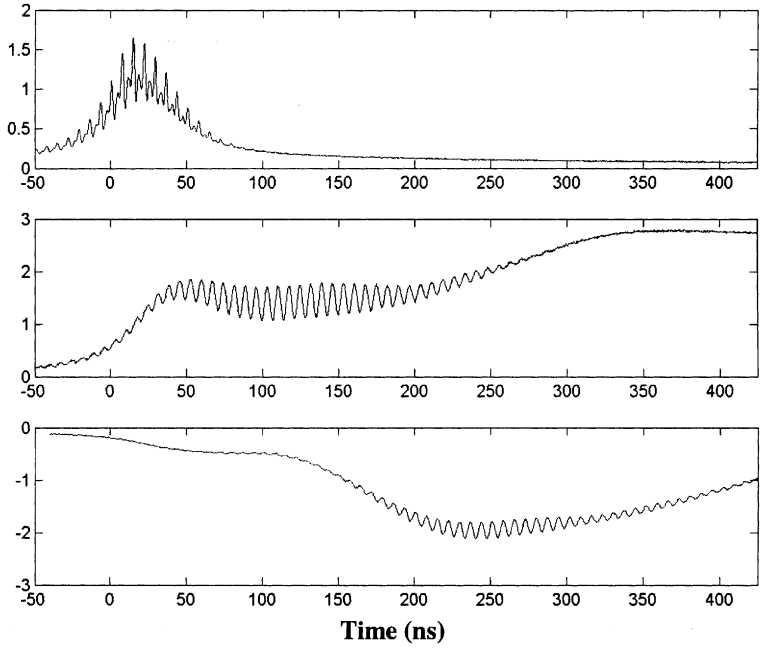

Fig. 2. Top: Temporal profile of laser pulse train recorded using a photodiode with a 1 GHz upper bandwidth. Middle: Acoustic pulse train measured 150 μm from the center of the source region. Bottom: Acoustic pulse train measured 675 μm from the source.

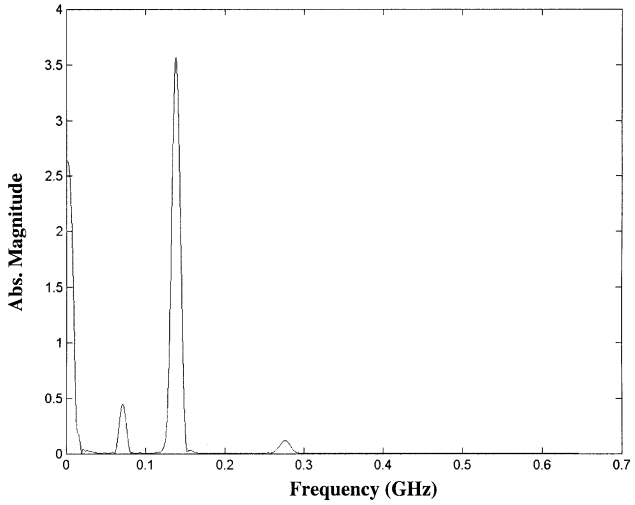

Fig. 3. Fouier amplitude spectrum: calibration signal is centered at 70 MHz and the fundamental and second harmonic are centered at 140 and 280 MHz respectively.

ematics is used to compute averages. In order to utilize the enhanced bit depth provided by averaging, all waveforms were averaged 400× resulting in a signal to noise ratio of approximately 200. A typical Fourier transform of the waveform data is presented in Fig. 3. The calibration signal at 70 MHz as well as the fundamental signal at 140 MHz and a signal at 280 MHz are clearly visible. In order to verify that the signal in the frequency range of the second harmonic is an artifact of elastic wave propagation and not due to some spurious source originating from the transduction or recording process, a series of signals were recorded as a function of laser intensity.

The amplitudes of the fundamental, A_1, and the second harmonic, A_2, as a function of laser intensity are shown in Fig. 4. The fundamental scales in a linear

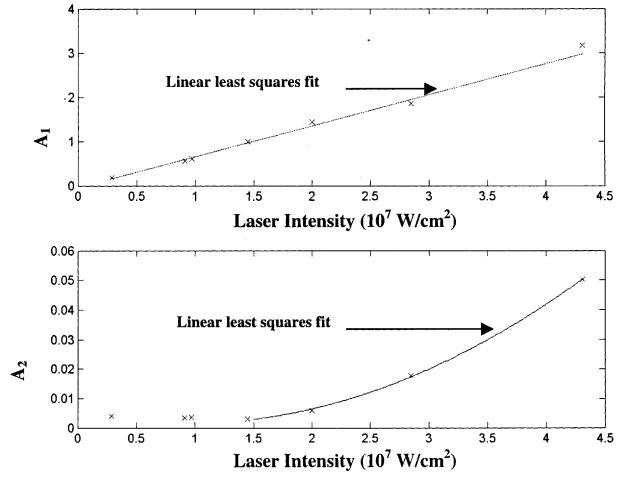

Fig. 4. Top: Amplitude of the fundamental as a function of laser intensity. Bottom: Amplitude of the second harmonic as a function of amplitude.

fashion with intensity. The first few data points in the graph for the second harmonic correspond to a signal to noise ratio that is less than one, and hence represent noise. The data points from about 1.5 MW/cm^2 to about 4.5 MW/cm^2, scale with the square of the intensity in accordance with nonlinear generation due to elastic wave propagation. It was observed that the onset of ablation occurs for integrated laser intensities greater than 4.5 MW/cm^2. Furthermore, the narrow band character of the signal starts to deteriorate in the ablative regime. One possible explanation is that the latter pulses in the pulse train are partially absorbed and or refracted by the plasma generated during the ablation process.

The ratio of the second harmonic to the fundamental amplitude as a function of scan distance is presented in Fig. 5. This data was obtained by fixing the

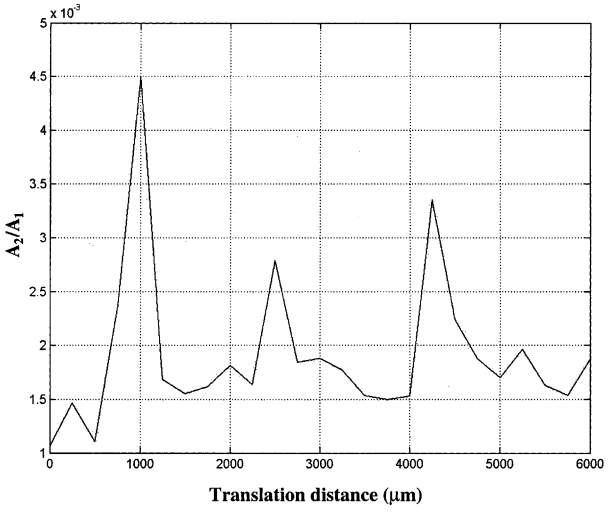

Fig. 5. Ratio of the second harmonic to the fundamental amplitude as a function of scan distance. The source-receiver separation is approximately 400 μm.

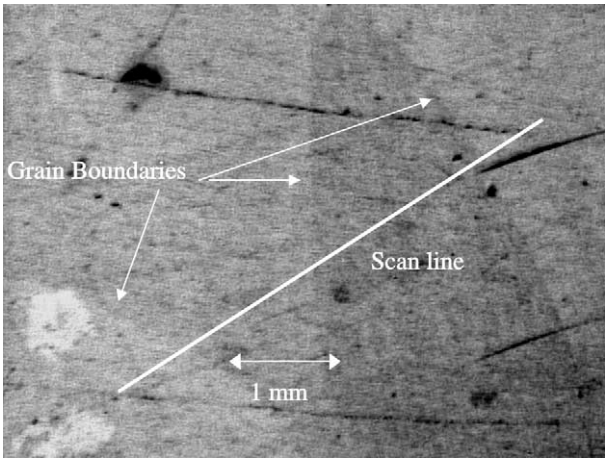

Fig. 6. Digitally enhanced photograph of the sample, showing the grain structure along the scan line.

source-receiver separation and scanning the sample in 125 μm steps. A photograph of the scanned region is shown in Fig. 6. The scan distance is approximately 3 mm, represented by 24 data points. The data shown in Fig. 5 reveals large jumps in the amplitude ratio which correspond to grain boundaries. The origin of these spikes in the amplitude ratio is the subject of ongoing research. One possible explanation involves increased harmonic generation at the grain boundaries due to lattice defects such as voids and dislocations. Another possible explanation entails harmonic generation due to surface defects at the grain boundaries imposed by the etching process.

4. Conclusion

Issues related to enhanced spatial sensitivity to spatial variations in elastic nonlinear behavior have been discussed. Preliminary results for surface acoustic waves generated at a center frequency of 140 MHz have been presented. Acoustic scans across the sample show large jumps in the ratio of the second harmonic to the fundamental amplitude, which might be indicative of sensitivity to defects such as dislocations and voids present at the grain boundary.

Acknowledgements

The authors gratefully acknowledges R.N. Wright for helpful suggestions and for supplying samples suitable for the experiment outlined in this paper. This work was sponsored by the US Department of Energy, Office of Science, Office of Basic Energy Sciences, Engineering Research Program under DOE Idaho Operations Office Contract DE-AC07-99ID13727.

References

[1] O. Buck, in: D.O. Thompson, D.E. Chimente (Eds.), Review of Progress in QNDE 9B, Plenum Press, New York, 1990, pp. 1677–1684.
[2] L.A. Ostrovsky, J. Acoust. Soc. Am. 90 (1991) 3332.
[3] T. Suzuki, A. Hikata, C.J. Elbaum, J. Appl. Phys. 35 (1964) 2761.
[4] J.H. Cantrell, W.T. Yost, Philos. Mag. 69 (1994) 315.
[5] C.A. Cain, J. Acoust. Soc. Am. 80 (1986) 28.
[6] E.A. Zabolotskaya, J. Acoust. Soc. Am. 91 (1992).
[7] C. Edwards, A.C. Bushell, S.B. Palmer, H. Nakano, Nondestr. Test Eval. 10 (1992) 15.
[8] A.D.W. McKie, Ph.D. Dissertation, University of Hull, 1987.